

PAPER • OPEN ACCESS

## The failure evolution characteristic of the arched structure under blast loading

To cite this article: Qindong Lin *et al* 2023 *J. Phys.: Conf. Ser.* **2535** 012020

View the [article online](#) for updates and enhancements.

### You may also like

- [Analysis on the Selection of Prefabricated Box-Shaped Steel Grid-Concrete Composite Thin-Shell Roof Structure](#)  
Cheng Hong, Jiaying Yu, Baohua Zhang et al.
- [Parametric resonance of bi-directional axial loads shallow arch microresonators](#)  
Fehmi Najar, Hassen M Ouakad, Abdallah Ramini et al.
- [Simultaneous Detection of Flare-related Decaying and Decayless Kink Oscillations Using Jerk-aware Motion Magnification](#)  
Xiaowei Guo, Bo Liang, Song Feng et al.

# The failure evolution characteristic of the arched structure under blast loading

Qindong Lin<sup>1</sup>, Chun Feng<sup>2</sup>, Yulei Zhang<sup>1\*</sup>, Yundan Gan<sup>1</sup> and Jianfei Yuan<sup>1</sup>

<sup>1</sup>Xi'an Modern Chemistry Research Institute, Xi'an, Shaanxi, 710065, China

<sup>2</sup>Institute of Mechanics, Chinese Academy of Sciences, Beijing 100190, China

Corresponding author: 13319237513@163.com

**Abstract.** Aiming at the arched structure in the field of defense engineering, it is of significant military value and theoretical innovation to investigate the failure mode and evolution characteristic of the arched structure under blast loading. First, a full-time simulation of the underground arched structure under blast loading is carried out. Then, the displacement evolution characteristic of the arched structure is studied. Finally, the crack evolution characteristic of the arched structure is studied. The numerical simulation indicates that the displacement of concrete near the midpoint of the straight wall at the right side is largest. The rock mass on the outside of the right arch segment and the middle arch segment collapses the most seriously. As the time increases, the fracture ratio continues to increase, and the fractured interface appearing during the explosion stage accounts for 43.65% of the total fractured interface. The damage degree of concrete of the straight wall and the arch segment at the right side is the most severe, and the rock mass mainly undergoes shear fracture.

## 1. Introduction

In the field of defense engineering, the arched structure has become a common structural form of underground defense engineering due to its excellent mechanical property and convenient engineering construction. Therefore, it is of great military value to explore the damage mode and evolution law of the concrete arched structure under blast loading.

The distribution of blast loading directly affects the damage mode and dynamic response of the structure. For the external pressure distribution law and load coefficient of the underground arched structure under blast loading, scholars have conducted a great deal of work and obtained a series of research achievements [1, 2]. To more accurately investigate the damage evolution law and dynamic mechanical response of the underground arched structure, scholars conduct lots of experimental studies and generalize the failure law [3, 4].

Due to the rapid development of computer technology, many scholars investigated the damage characteristic of the concrete arched structure based on numerical simulation. For the 45° side top blast, Huo et al. [5] investigated the damaging effect of the underground arched structure with the reinforced concrete wall. Regarding the top explosion, Kong et al. [6] conducted a numerical simulation of the underground arched structure with different detonating distances and rock types and established the influence law between the span and rock type. Liu et al. [7] studied the effects of charge quantity and blasting distance on the loading distribution of the arched structure. Regarding the curved masonry structure, Masi et al. [8] studied the impact of microscopic mechanical parameter on the macroscopic response of structure. Sun et al. [9] explored the failure mode and maximum stress change curve of the



underground arched structure with different spans.

Although a great deal of numerical research on the failure mode of the underground arched structure has been done, the process of structure that transforms from continuous stage to discontinuous stage is rarely studied due to the continuum-based numerical method. This paper aims to study the dynamic response (i.e., fracture characteristic, displacement characteristic) of the underground arched structure under blast loading using the continuum-discontinuum element method. The research results are important to guide the designed parameter of the arched structure and improving the resistance to military strikes or accidental explosions.

## 2. Numerical simulations

According to the Lagrangian energy system theory, the continuum-discontinuum element method (CDEM) is proposed. The explicit iterative solution is achieved by the dynamic relaxation method, which can improve the applicability of solving large deformation problems [10]. Based on the CDEM numerical algorithm, many researchers investigate the mechanical response process of structure under dynamic loading, and the experimental results verify the accuracy of CDEM. Therefore, CDEM is adopted to simulate the mechanical response of the arched structure under blast loading, and the evolution characteristic of fracture and displacement is studied.

### 2.1 Basic information

Figure 1 plotted the numerical model of the arched structure and rock mass. The distance from arched structure to the bottom boundary of rock mass is 30 m, the distance from arched structure to the left boundary of rock mass is 60 m. The distance from explosive to the bottom boundary is 50 m, and the distance from explosive to the left boundary is 100 m. The thickness of the concrete wall is 0.8 m, the horizontal distance of arched structure is 9.6 m, and the vertical distance of arched structure is 9.8 m. The parameters of JWL equation of state is listed in Table 1, and it is used to simulate the explosion process.

The numerical simulation is divided into two stages, which aims to simulate the dynamic response of arched more accurately. The static simulation stage is used to simulate the mechanical response of arched structure and rock mass under the gravity is simulated. During the dynamic simulation stage, the non-reflecting boundary is applied at the left boundary and bottom boundary, and the dynamic response of the arched structure and rock mass under blast loading is simulated.

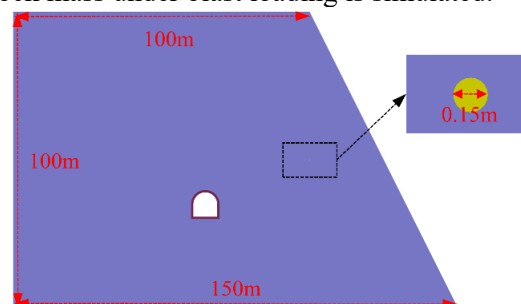


Figure 1. Model of arched structure and rock mass

Table 1. Mechanical parameters of JWL equation of state

Material	Charge density (kg/m <sup>3</sup> )	Internal energy (J/m <sup>3</sup> )	CJ pressure (Pa)	Detonation velocity (m/s)
TNT	1630	7e9	21e9	6930

### 2.2 Numerical results

Using the CDEM numerical method, the dynamic response of the arched structure and rock mass under blast loading is obtained, and the displacement characteristic and fracture characteristic are quantitatively analyzed.

### 2.2.1 Characteristic of displacement

Figure 2 plots the resultant displacement nephograms at different moments, and only the arched structure and rock mass near the arched structure are plotted.

From Figure 2(a), it is observed that the concrete at the right and bottom boundaries of the arched structure moves under the shock wave, and the displacement of concrete at the right boundary is much larger than that of concrete at the bottom boundary. For the concrete at the right boundary, not only the concrete at the straight-wall segment moves towards the center area of the arched structure, but also part of the concrete at the right arch segment moves. The maximum value of displacement appears near the midpoint of the straight wall. Regarding to the concrete at the bottom boundary, although the fracture degree is weaker than that of concrete at the right boundary, the concrete in the middle part has been separated from the surrounding concrete.

When the time is 0.2 s, the concrete at the right straight wall is about to reach the left boundary, which gradually moves downward under the action of gravity, and part of them collides with the concrete at the bottom boundary. More concrete at the right arch segment occurs movement and fracture, and the cracked area expands to the middle of the arch segment.

When the time is 0.6 s, the concrete at right straight wall segment has reached the left boundary, and some concrete at the left boundary undergoes fracture and separation during the interaction process. The crack degree of concrete at the middle and right arch segment increases further, and the concrete begins to show a tendency to collapse completely. Due to the loss of support from the concrete wall, the rock on the right side and above the arched structure is going to collapse.

When the time is 1.0 s, The concrete at the right straight-wall segment, the right arch segment, and the middle arch segment has been severely destabilized and completely loses the load-bearing capacity. The collapsed rock area continues to expand, and the collapse of rock on the outside of the right arch segment and the middle arch segment is the most serious.

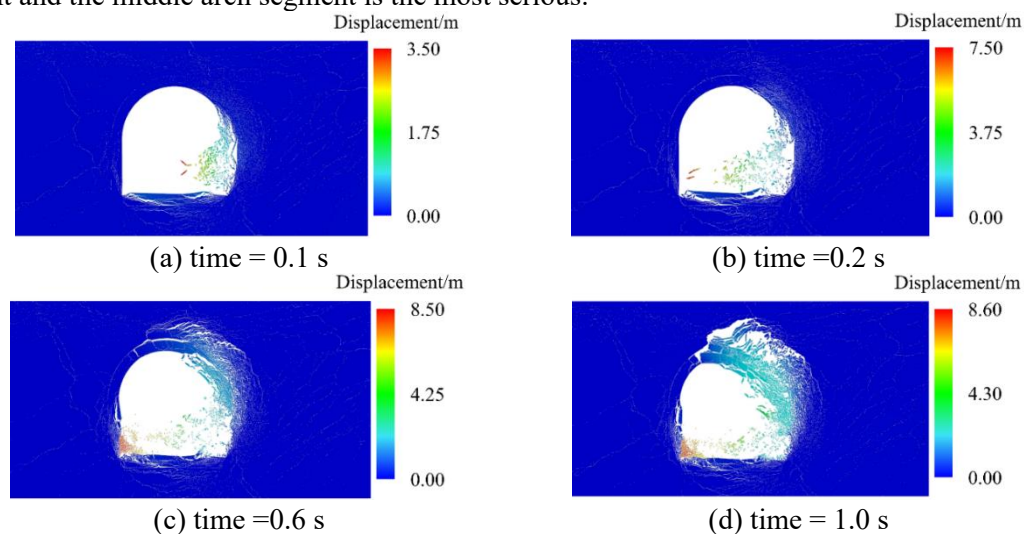


Figure 2. Resultant displacement nephograms

### 2.2.2 Characteristic of fracture

Figure 3 plots the change trend of fracture ratio  $\alpha$ . As the time increases, the fracture ratio  $\alpha$  continuous to increase. Three inflection points are located on the curve, which is point A, point B and point C. At the OA stage, the fracture ratio is zero at the initial moment because the shock wave has not yet reached the arched structure. Then a great deal of interface between the concrete elements satisfies the fracture criterion and cracks under the strong impact action of the shock wave, which results in the sharp increase in the fracture ratio  $\alpha$ . Subsequently, despite the disappearance of explosion gas, many interfaces still crack under the shock wave, and  $\alpha$  continues to increase rapidly. At the AB stage, the impact action of the shock wave is weakened significantly, and the growth trend of  $\alpha$  decays. At the BC stage,  $\alpha$  increases sharply again because the concrete at the right boundary reaches the left boundary, and some interface

at the left boundary cracks under the impact action. In the CD range, the concrete wall is gradually destabilized, and some interface cracks during the collapse process, resulting in a slow increase in the fracture ratio  $\alpha$ . According to the explosive characteristic, the time-history curve is divided into the explosion stage and the post-explosion stage. The fracture ratio  $\alpha = 17.16\%$  at the end moment of the explosion stage, and the fracture ratio  $\alpha = 39.31\%$  at the end moment of the post-explosion stage. It is concluded that the fractured interface appearing during the explosion stage accounts for 43.65% of the total fractured interface.

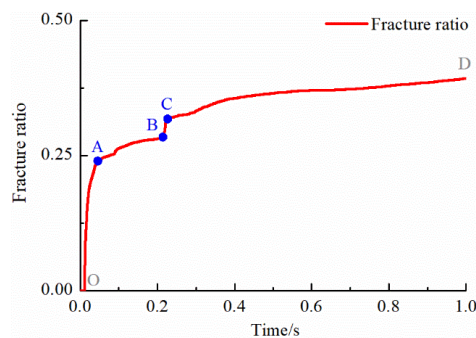


Figure 3. The change trend of fracture ratio  $\alpha$

To further study the spatial distribution characteristic and fracture type, Figure 4 plots the fracture nephograms near the arched structure.

When the time is 0.01 s, the explosion shock wave reaches the arched structure. Since the compressive stress wave is transformed into the tensile stress wave at the free face, the interface at the right arch segment mainly occurs tensile fracture.

When the time is 0.02 s, some interface at the four boundaries of arched structure cracks, and both of the tensile fracture and shear fracture appears. The concrete at the right straight wall and the right arch segment undergoes the most severe damage, and the crack type of interface is mainly shear fracture. The rock mass on the right side and above the arched structure also cracks, which mainly undergoes tensile fracture.

At  $t = 0.2$  s, the crack degree of rock mass and concrete is further aggravated, and the newly cracked concrete interface is mainly located at the straight wall and arch segment. Although the rock above the arched structure has been severely damaged, it does not collapse because of the strong load-bearing capacity of the concrete wall.

When the time is 1.0 s, the concrete at the right boundary has reached the left boundary, some concrete interface at the left boundary cracks under the impact action, and most of the newly cracked interface undergoes shear fracture. Although the fracture degree of rock above the arched structure does not increase significantly, it collapses because the concrete at the right arch segment and the middle arch segment has been completely destabilized.



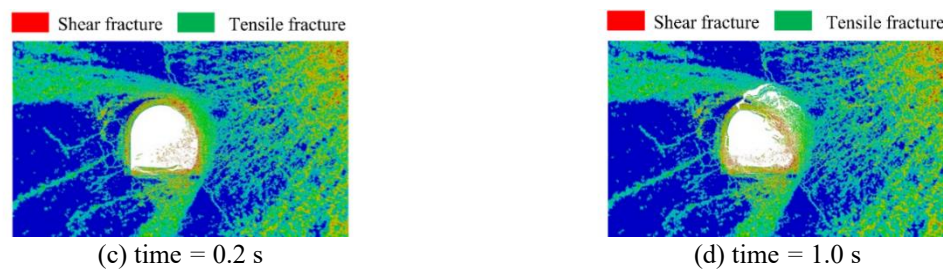


Figure 4. Crack nephograms near the arched structure

### 3. Conclusions

The fracture evolution characteristic and displacement evolution characteristic of the arched structure are studied. The following conclusions are drawn:

1) Under the explosion shock wave, the arched structure undergoes movement and fracture. The maximum value of displacement appears near the midpoint of wall. The collapse of rock mass above the right arch segment and the middle arch segment is the most serious.

2) As the time increases, the fracture ratio  $\alpha$  continuous to increase, and there are three inflection points appears on the curve. During the first and third periods,  $\alpha$  increases sharply, and it increases slowly during the second and fourth periods. The fractured interface appearing during the explosion stage account for 43.65% of the total fractured interface.

3) For the concrete interface, the crack degree of concrete at the right arch segment and the straight wall is severe, and most of the interface undergoes shear fracture. For the rock mass, the rock on the right side and above the arched structure mainly undergoes tensile fracture, with two tensile fracture zones around the arched structure.

The conclusions quantitatively characterize the deformation and fracture of the underground arched structure, which are important to guide its design and improve the resistance to military strikes or accidental explosions. Since the presence of steel reinforcement leads to a change in the mechanical response of the arched structure, the following research priority is on the dynamic mechanical response of the reinforced concrete arched structure and the correspondence between the mechanical response of the arched structure and the mechanical quantities of explosive.

### References

- [1] Huo, Q., Wangm W., Lium G.K. and Huang, Z.W. (2021) Numerical simulation research on load distribution law of underground arched structure with 45° side top blast. *Protective engineering*, 43: 11-18.
- [2] Ambrosini, D. and Luccioni, B. (2020) Effects of underground explosions on soil and structures. *Underground space*, 5: 324-338.
- [3] Liu, G.K, Liu, R.C., Wang, W., Wang, X. and Zhao, Q. (2021) Blast resistance experiment of underground reinforced concrete arch structure under top explosion. *Chinese journal of energetic materials*, 29: 157-165.
- [4] Chen, H. L., Zhou, J.N., Fan, H.L., Jin, F.N., Xu, Y., Qiu, Y.Y., Wang, P. and Xie, W. (2014) Dynamic responses of buried arch structure subjected to subsurface localized impulsive loading: experimental study. *International journal of impact engineering*, 65: 89-101.
- [5] Huo, Q., Wang, Y.P., Liu, G.K. and Wang, W. (2021) Failure mode and influencing factors of underground arched structure subjected to side top blast. *Acta armamentarii*, 42: 105-116.
- [6] Kong, D. Q., Sun, H.X., Kang, T. and Ma, T. (2014) The influence of rock characteristics on dynamic interaction between adjoining rock and structure subjected to blast loading. *Journal of air force engineering university (natural science edition)*, 15: 77-81.
- [7] Liu, G. K., Wang, W., Liu, R.C., Liu, J. and Kong, D.F. (2017) Numerical analysis of loading distribution on underground arch structure under close-in explosion. *Acta armamentarii*, 39: 102-107.

- [8] Masi, F., Stefanou, I., Berthier, V.M. and Vannucci, P. (2020) A discrete element method based-approach for arched masonry structures under blast loads. *Engineering structures*, 216: 110721.
- [9] Sun, H.X., Xu, J.Y., Zhu, G.F., Zhu, J. and Kang, T. (2013) The influence of span for deep underground arch structure on failure modes under blast loading. *Journal of air force engineering university (natural science edition)*, 14: 90-94.
- [10] Lin, Q.D., Li, S.H., Gan, Y.D. and Feng, C. (2022) A strain-rate cohesive fracture model of rocks based on lennard-jones potential. *Engineering fracture mechanics*, 259: 108126.